condensed matter

MDPI

Article

Substrate-Induced Proximity Effect in Superconducting Niobium Nanofilms

S.J. Rezvani [1,2,3,*,†], Andrea Perali [4], Matteo Fretto [2], Natascia De Leo [2], Luca Flammia [1,5], Milorad Milošević [5], Stefano Nannarone [3] and Nicola Pinto [1,2,*]

1 SuperNanoLab, School of Science and Technology, Physics Division, University of Camerino, via Madonna delle Carceri 9, 62032 Camerino, Italy; luca.flammia@unicam.it
2 Istituto Nazionale di Ricerca Metrologica (INRiM), Strada delle Cacce 91, 10135 Torino, Italy; fretto@inrim.it (M.F.); deleo@inrim.it (N.D.L.)
3 IOM-CNR Lab TASC Area Science Park, Basovizza Building MM, SS. 14, 34149 Trieste, Italy; Nannarone@iom.cnr.it
4 SuperNanoLab, School of Pharmacy, Physics Unit, University of Camerino, via Madonna delle Carceri 9, 62032 Camerino, Italy; andrea.perali@unicam.it
5 Department of Physics, University of Antwerp, Groenenborgerlaan 171, B-2020 Antwerp, Belgium; milorad.milosevic@uantwerpen.be
* Correspondence: rezvani@lnf.infn.it (S.J.R.); nicola.pinto@unicam.it (N.P.)
† Current address: INFN—Laboratori Nazionali di Frascati, Via Enrico Fermi, Frascati, 40, 00044 Roma, Italy.

Received: 18 November 2018; Accepted: 26 December 2018; Published: 30 December 2018

Abstract: Structural and superconducting properties of high-quality niobium nanofilms with different thicknesses are investigated on silicon oxide (SiO_2) and sapphire substrates. The role played by the different substrates and the superconducting properties of the Nb films are discussed based on the defectivity of the films and on the presence of an interfacial oxide layer between the Nb film and the substrate. The X-ray absorption spectroscopy is employed to uncover the structure of the interfacial layer. We show that this interfacial layer leads to a strong proximity effect, especially in films deposited on a SiO_2 substrate, altering the superconducting properties of the Nb films. Our results establish that the critical temperature is determined by an interplay between quantum-size effects, due to the reduction of the Nb film thicknesses, and proximity effects. The detailed investigation here provides reference characterizations and has direct and important implications for the fabrication of superconducting devices based on Nb nanofilms.

Keywords: niobium thin film; proximity effects; superconductivity; quantum confinement

1. Introduction

Superconductivity has been recently shown to survive even in extremely confined nanostructures such as metal monolayers [1]. Preserving a superconducting state in ultra-thin films can be achieved by nanofabrication techniques and withstand multiple cooling cycles. However, control over the superconducting properties of metallic ultra-thin films are of utmost importance in realization of quantum devices, such as Josephson junctions, nano Superconducting QUantum Interference Devices (SQUIDs), mixers and single photon detectors [2–7]. Hence, a systematic investigation on their properties and their optimization at reduced dimensionality can leads to an ideal platform to control electronic confinement and novel multi-condensate superconductivity near a Lifshitz transition where it has been proposed that the interplay between a first condensate in the Bose Einstein condensate (BEC) and a second condensate in the Bardeen-Cooper-Schrieffer (BCS) and Bose Einstein condensate (BCS/BEC) crossover regime can give high temperature superconductivity [8–13].

Niobium is a ubiquitous material for superconducting thin films and its performance is known to increase when epitaxy conditions can be reached [14]. On the other hand, the proximity effect occurs when a superconductor is placed in contact with non-superconducting materials. The resulting critical temperature of the superconductor in this case is suppressed and signs of weak superconductivity are induced in non-superconducting materials. Superconducting correlations are induced in the normal side, up to a distance where the electron and hole lose phase-coherence [15]. Furthermore, it is shown that the substrate induced surface states can play a significant role in electronic properties of nanostructures [16,17]. However, a combined electrical and structural study on the presence and role of the proximity effect induced by the substrate on the superconducting properties of Nb ultra-thin films is lacking.

In this work we report an extended experimental investigation of the superconducting to normal state transition in Nb nanofilms, with a thickness in the range 9 nm to 80 nm, deposited on SiO_2 and Al_2O_3 substrates. A detailed analysis of several superconducting properties of these Nb nanofilms has been reported in [18]. The main microscopic parameters characterizing the normal and the superconducting state of these films were investigated based on recent models. We have explored the important role played by the substrate on the fundamental properties of the Nb nanofilms. Our study establishes the existence of an interplay between quantum-size and proximity effects at the substrate interface [19,20].

2. Experiment

Nanofilms of Niobium have been deposited at room temperature on thermally oxidized Si wafer (silicon oxide SiO_2 with thickness: 300–500 nm) and on sapphire, in an ultra-high vacuum dc sputtering chamber, with a base pressure $\approx 2 \times 10^{-9}$ mbar. Films were deposited with thicknesses in the range from 9 nm to 80 nm with a constant deposition rate of 0.65 nm/s. Scanning electron microscopy (SEM) analysis has been carried out on some films by a FEI Quanta^{TM} 3D FIB. Electronic transport properties of samples were measured using a Hall bar geometry, 1–2 cm long and 10 μm and 50 μm wide. The resistivity, $\rho(T)$, was measured as a function of the temperature, in the range 4–300 K, by a He closed cycle cryostat (ARS mod. DE-210S) equipped with two silicon diode thermometers (Lakeshore mod. DT-670). Resistivity has been measured sourcing a constant current (Keithley mod. 220), monitored by a pico-ammeter (Keithley mod. 6487) and a multimeter measuring the voltage drop (Keithley mod. 2000). The current was sourced in the range 1–50 μA. Further details can be found in the reference [18]. The X-ray absorption measurements were carried out on oxygen K-edge on an 80 nm thick Nb film at IOM-CNR, BEAR beam line at Elettra synchrotron radiation center (Trieste, Italy) [21,22]. The beam line operates in the 2.8–1600 eV (443–0.775 nm) spectral region, delivering polarized light of selectable ellipticity from nearly linear to elliptical (see Figure 1).

The samples were mounted in the experimental chamber after the divergence selector slits with a base pressure of 1×10^{-9} mbar and were positioned at 45° with respect to the incident beam (with a solid angle of ∼0.8 strad). A reference current was measured simultaneously to the measurement to normalize the measured spectra to the variation of the photon intensities, while the incident beam was measured after removal of the sample from the experimental chamber. The measurements were carried out in total fluorescence mode to achieve a mean probing depth of ∼100 nm [23] to include both Nb film and substrate interface. The overall error of measurement on fluorescence yield was estimated of the order of 1%.

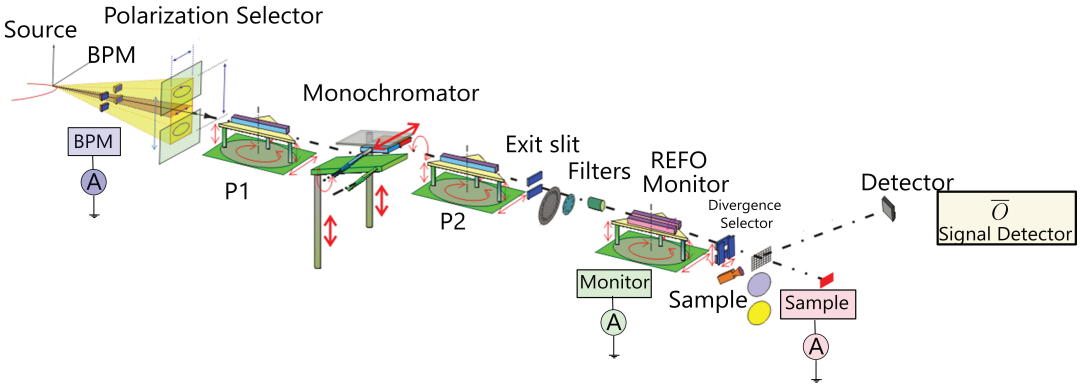

Figure 1. BEAR beam line set up [24]. The XAS measurements were carried out in the experimental chamber in two Total Electron Yield (TEY) and Total Fluorescence Yield (TFY) modes in which for the first the emission current was measured from the sample and the fluorescence signal was measured for the later one. Both signals were normalized to the signal from the monitor for the correction of the optical apparatus absorption and to the incident beam.

3. Results and Discussion

The resistivity of the Nb films ρ and its temperature dependence was investigated as a function of the film thickness, d (see Figure 2a). Results show (Table 1) that the superconducting transition temperature, T_C, decreases quite abruptly as d is progressively reduced while the $\rho(T)$ curves shift upwards. At a thickness equal to 80 nm our films resistivity approaches the expected Nb bulk value of 15 μΩcm [25,26]. While the superconducting properties of the Nb film is influenced by the lattice parameters of the deposited film as well the grain sizes in the polycrystalline film [27,28], the decrease of the film resistivity in thicker films may suggest a gradual reduction of the film defectivity via atomic rearrangement or increase of the grain size [29–31]. An additional effect that could play a role in the suppression of Nb critical temperature, for decreasing thickness, is based on changes in the density of states (DOS) due to the quantization of the electronic motion, while the electron-phonon coupling responsible for Cooper pairing remains almost unaffected by reducing the thickness, as found in Ref. [32]. On the other hand, the Nb nanofilms of Ref. [32] have been fabricated in a such a way to form a granular structure (grain size ranging from 5 to 60 nm), by means of a suitable control of the deposition parameters. Under this condition, the quantum-size effects, and the corresponding reduction of the DOS (and hence of the critical temperature) will be amplified by the nano-grain strong confinement.

Table 1. The experimentally measured properties of different Nb nanofilms. From left to right: Substrate; Film thickness; Critical temperature T_C; Superconducting transition width, ΔT_C; Resistivity at 10K and mean-free path (l).

Substrate	Thickness (nm)	T_C (K)	ΔT_C (mK)	ρ_{10} (μΩcm)	l (nm)
SiO_2	9.0	6.46	50	64.70	0.58
SiO_2	11.0	6.53	65	48.90	0.77
SiO_2	12.0	6.47	30	71.70	0.52
SiO_2	13	6.84	19	38.44	0.98
SiO_2	19.5	7.48	49	16.56	2.26
SiO_2	22.5	7.89	44	11.25	3.33
SiO_2	25	8.40	15	9.23	4.06
SiO_2	28.0	8.51	28	8.45	4.44
SiO_2	28.0	7.97	65	12.05	3.11
SiO_2	34.0	8.58	16	6.63	5.66
SiO_2	35.0	8.519	29	6.11	6.14
SiO_2	50.0	8.63	20	6.87	5.46
SiO_2	80.0	9.13	11	4.21	8.91
Al_2O_3	13.5	7.313	75	-	-
Al_2O_3	19.5	7.91	35	12.08	3.10
Al_2O_3	22.5	8.11	28	8.90	4.21

Compared to the data reported in the literature, the T_C of Nb films deposited on silicon oxide (SiO_2) show lower values for smaller thicknesses. On the other hand, while in general T_C shows a strong decreasing behavior as a function of film thickness, Nb films deposited on sapphire consistently demonstrate higher T_C compared with the ones deposited on SiO_2 (Figure 2a). Film residual resistivity at $T = 10$ K (i.e., ρ_{10}, see Figure 2c) also show an increasing trend, by reduction of thickness, while this increase is less pronounced for those deposited on sapphires. The charge carriers mean-free path l , was estimated from the residual resistivity (ρ_{10}) assuming the constancy of the product $\rho l = 3.75 \times 10^6$ $\mu\Omega cm^2$ [Ref. [30] and references there in] here ρ assumed to be equal to the measured ρ_{10}, i.e., the lowest resistance value of Nb films in the normal state. We found l values ranging from $\approx$1 nm, at the lower thicknesses, to $\simeq$9 nm at $d = 80$ nm (Figure 2d). The results also show a higher mean-free path (l values) for the Nb films deposited on sapphire. The width of the superconducting transition, ΔT_C, also exhibits an increasing trend from 15 mK at 80 nm to 80 mK for 10–20 nm films (Figure 2b). While ΔT_C in our samples show lower values compared to those reported in the literature, suggesting a relatively higher quality films [29], the transition width of the Nb films on sapphire are relatively lower. These results suggest an enhancement of the superconducting properties on sapphire substrate that can be associated with two distinct effects. In detail, while the formation of an oxidized Nb (i.e., NbO_x) layer [33] at the interface film-substrate, becomes progressively stronger with the reduction of d and it results effective for both type of substrate, the deposition on sapphire induces less defects in the Nb film since sapphire lattice parameter and thermal dilatation coefficients match rather well with Nb [14]. This oxide layer reduces the effective Nb film thickness leading to a lower T_C. Such a contribution is largely reduced on sapphire substrates as can be seen in Figure 2d. Moreover, NbO_x layer, being a conductive system of electrons in its normal state, can sink Cooper pairs from the superconducting Nb nanofilm, suppressing the condensate fraction and reducing the T_C via proximity effect. This phenomenon dominates as the thickness of the Nb film is reduced with the NbO_x layer becoming a sizable fraction of the Nb film thickness, similar to the behavior of T_C in our films. The lower defectivity in the film matrix agrees with the higher l values for Nb deposited on sapphire.

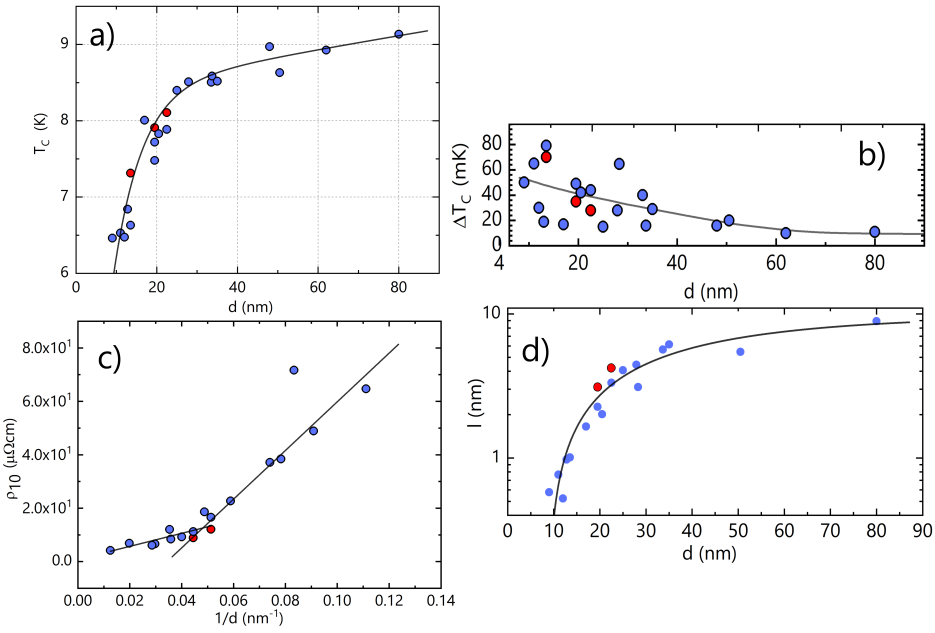

Figure 2. Nb film thickness dependence of: (**a**) T_C; (**b**) width of the superconducting transition; (**c**) residual resistivity; (**d**) mean-free path at 10 K. These last have been derived from the resistivity values measured at the same temperature (i.e., ρ_{10}). Blue and red filled symbols, refer to deposition carried out on SiO_2 and sapphire substrates, respectively.Continuous lines are guides for eyes.

The oxide formation at the Nb/substrate interface can occur from oxygen atoms diffusion into the metallic film due to presence of defective bonds while on the surface due to the exposure to the air. In order to investigate the formation of such oxide layers, at Nb surface and its interface with substrate, we carried out detailed experiments by X-ray absorption near edge structure (XANES) measurements in Total Fluorescence Mode (TFY). This technique, with a Mean Probing Depth (MPD) of ∼100 nm is perfectly suitable to reach the interface layer of an 80 nm thick Nb film [23,34]. The TFY spectra of the films on silicon oxide (SiO_2) and sapphire at oxygen K-edge are reported in Figure 3a,b along with the reference spectra of SiO_2, Al_2O_3, Nb_2O_5 and NbO. As shown clearly in the figure, samples on both substrates show two main features at around 531 and 535 eV (B and C) corresponding to the stable Nb_2O_5 phase (B), while for the sample on SiO_2 the component C is broadened due to the signal from the substrate itself. Furthermore, the increased intensity of the component C of the sample on sapphire and the broad component (D) as well, can be associated with the contribution of the sapphire substrate. These results confirm the formation of a major Nb_2O_5 phase on both samples including the superficial layer.

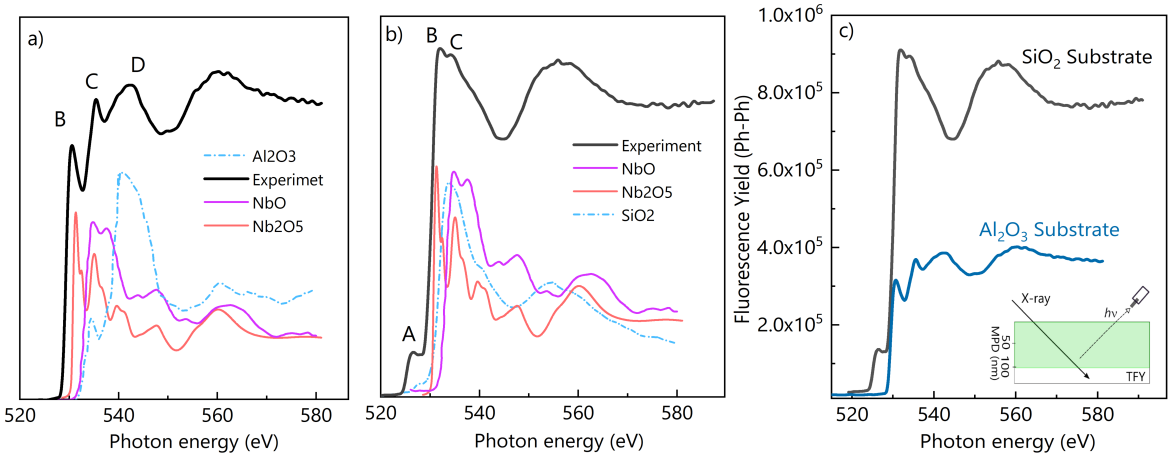

Figure 3. X-ray absorption near edge (XANES) spectra of the O K-edge of the films deposited on the (**a**) sapphire and (**b**) silicon oxide (SiO_2) in TFY mode along with the reference spectra of SiO_2, Al_2O_3, Nb_2O_5 and NbO. (**c**) normalized florescence yield, measured on samples on SiO_2 and sapphire along with the schematic of the TFY MPD.

However, the TFY spectra of the Nb/SiO_2 film exhibits an extra pre-edge structure (A) that cannot be corroborated neither with usual niobium oxides phases, such as Nb_2O_5 or NbO, nor with the SiO_2 substrate itself and hence, signifies formation of a semi metallic Nb oxide (e.g., NbO_x). This semi metallic layer may induce a strong proximity effect, potentially sinking Cooper pairs from the superconducting Nb nanofilms and then leading to a strong reduction of the condensate fraction. Moreover, it can be seen that the normalized signal of the Nb/SiO_2 sample (Figure 3c) shows significantly higher intensity compared to that of Nb/Al_2O_3. This indicates higher concentration of the oxygen absorbers in case of Nb/SiO_2 film that can be associated with the formation of a thicker oxide film. The thicker oxide layer can reduce the effective thickness of the superconducting Nb film resulting in a further alteration of the superconducting properties. A detailed analysis of the formation of the interfacial and superficial oxides layers on the superconducting Nb films is the object of a forth coming paper Ref. [35].

Finally, to investigate the T_C suppression due to the proximity effect induced by superficial/interfacial oxide layers, an approach by McMillan [36] was employed (Equation (1)). In the approach $\alpha = d_N N_N(0)/N_S(0)$, d_N is an effective thickness of the conductive layer at the interface; $T_{C0} = 9.22$ K is the bulk T_C of Nb and $T_D = 277$ K is the Debye temperature. The quantities

$N_N(0)$ and $N_S(0)$ are the DOS in the normal (N) and superconducting (S) layers, respectively and here assumed to be equal [18].

$$T_C = T_{C0}\left(\frac{3.56T_D}{T_{C0}\pi}\right)^{-\alpha/d} \quad (1)$$

Fitting our data using Equation (1) for $T_C(d)$ we obtain a value of $\alpha = 0.96 \pm 0.04$ nm (Figure 4) for films on SiO_2 and $\alpha = 0.84 \pm 0.02$ nm for films on sapphire. However, the α value for the films deposited on sapphire are calculated from few points available in our experiment. These results are in a good agreement with the TFY results and can reasonably correspond to two different thin oxide layers induced by the substrates, resulting in a thinner oxide layer when Nb films are deposited on sapphire. Furthermore, in the presence of an overall suppression of $T_C(d)$ due to proximity effect, the fitting function given by Equation (1) can be subtracted from the data set in order to amplify the visibility of probable oscillations of T_C for decreasing d due to the incipient quantum-size effects and shape resonances associated with the electronic confinement in the perpendicular direction. Subtracting the fit from the experimental data, we observe progressively increasing residual T_C oscillations by decreasing d, with amplitude of 5% in the thinnest films, comparable to the theoretical predictions for Pb and Al nanofilms [37].

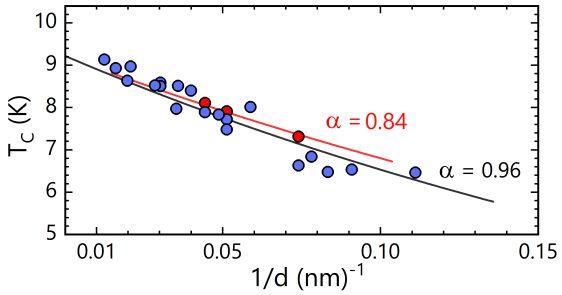

Figure 4. Superconducting transition temperature as a function of the reciprocal film thickness. Blue circles are Nb films on SiO_2 substrate and red circles on sapphire substrate. Continuous line is least-squares fit, using Equation (1). The effective thickness of the normal layer (in nm) is represented by the corresponding α value.

4. Conclusions

In this work we have experimentally clarified the microscopic mechanism causing the suppression of the critical temperature in superconducting Nb nanofilms for thicknesses between 9–80 nm. We have investigated the effects of the substrate (SiO_2 and sapphire) on the superconducting properties of thin Nb films via structural, electrical, and superconducting analysis. We have demonstrated the key role played by the substrate in improvement of the superconducting properties of the nanofilms. It is shown that this improvement can be the result of different effects such as the lower defectivity of Nb deposited on sapphire and formation of a semi metallic oxide layer at the interface with the SiO_2 substrate, observed by XANES spectroscopy. The XANES results also indicate a higher concentration of oxide in Nb films on SiO_2 substrates that may suggest a higher thickness of oxide layers. The higher thickness of the oxidized layers may lead to a lower effective thickness of the Nb films altering their superconducting properties. Our results point towards a significant contribution of proximity effect in the superconducting properties of the films, particularly for the films on SiO_2. We were able to disentangle the detrimental proximity effects from the quantum-size effects in T_C, demonstrating the existence of quantum-size oscillations and amplification of the critical temperature in Nb nanofilms due to the quantum confinement, an effect which was not yet observed up to now in Nb.

Author Contributions: S.J.R, N.P. and A.P. conceived the experiments. M.F. and N.D.L. fabricated samples. N.P., S.J.R., M.F. and S.N. conducted the experiments, N.P., A.P., L.F. and M.M. analyzed the results. All authors reviewed the manuscript.

Funding: This project was financially supported by University of Camerino, FAR project CESEMN.

Acknowledgments: The authors would like to thank A. Giglia and K. Koshmak for their assistance in X-ray Absorption Spectroscopy measurements and L. Pasquali for constructive discussions.

Conflicts of Interest: The authors declare no conflict of interest.

References

1. Zhang, T.; Cheng, P.; Li, W.J.; Sun, Y.J.; Wang, G.; Zhu, X.G.; He, K.; Wang, L.; Ma, X.; Chen, X.; et al. Superconductivity in one-atomic-layer metal films grown on Si(111). *Nat. Phys.* **2010**, *6*, 104. [CrossRef]
2. Delfanazari, K.; Puddy, R.K.; Ma, P.; Yi, T.; Cao, M.; Gul, Y.; Farrer, I.; Ritchie, D.A.; Joyce, H.J.; Kelly, M.J.; et al. Proximity induced superconductivity in indium gallium arsenide quantum wells. *J. Magn. Magn. Mater.* **2018**, *459*, 282–284. [CrossRef]
3. Sarma, S.D.; Hui, H.Y.; Brydon, P.M.; Sau, J.D. Substrate-induced Majorana renormalization in topological nanowires. *New J. Phys.* **2015**, *17*, 075001. [CrossRef]
4. Delfanazari, K.; Puddy, R.K.; Ma, P.; Yi, T.; Cao, M.; Gul, Y.; Farrer, I.; Ritchie, D.A.; Joyce, H.J.; Kelly, M.J.; et al. On-Chip Andreev Devices: Hard Superconducting Gap and Quantum Transport in Ballistic Nb–In0.75Ga0.25As-Quantum-Well–Nb Josephson Junctions. *Adv. Mater.* **2017**, *29*, 1701836. [CrossRef] [PubMed]
5. Savinov, V.; Delfanazari, K.; Fedotov, V.A.; Zheludev, N.I. Giant nonlinearity in a superconducting sub-terahertz metamaterial. *Appl. Phys. Lett.* **2016**, *108*, 101107. [CrossRef]
6. Semenov, A.; Engel, A.; Il'in, K.; Gol'tsman, G.; Siegel, M.; Hübers, H.W. Ultimate performance of a superconducting quantum detector. *Eur. Phys. J. Appl. Phys.* **2003**, *21*, 171–178. [CrossRef]
7. Karasik, B.S.; Gaidis, M.C.; McGrath, W.R.; Bumble, B.; LeDuc, H.G. Low noise in a diffusion-cooled hot-electron mixer at 2.5 THz. *Appl. Phys. Lett.* **1997**, *71*, 1567–1569. [CrossRef]
8. Mazziotti, M.V.; Valletta, A.; Campi, G.; Innocenti, D.; Perali, A.; Bianconi, A. Possible Fano resonance for high-T c multi-gap superconductivity in p-Terphenyl doped by K at the Lifshitz transition. *Europhys. Lett.* **2017**, *118*, 37003. [CrossRef]
9. Cariglia, M.; Vargas-Paredes, A.; Doria, M.M.; Bianconi, A.; Milošević, M.V.; Perali, A. Shape-Resonant Superconductivity in Nanofilms: from Weak to Strong Coupling. *J. Supercond. Novel Magn.* **2016**, *29*, 3081–3086. [CrossRef]
10. Innocenti, D.; Poccia, N.; Ricci, A.; Valletta, A.; Caprara, S.; Perali, A.; Bianconi, A. Resonant and crossover phenomena in a multiband superconductor: tuning the chemical potential near a band edge. *Phys. Rev. B* **2010**, *82*, 184528. [CrossRef]
11. Guidini, A.; Perali, A. Band-edge BCS-BEC crossover in a two-band superconductor: physical properties and detection parameters. *Supercond. Sci. Technol.* **2014**, *27*, 124002. [CrossRef]
12. Bianconi, A.; Innocenti, D.; Valletta, A.; Perali, A. Shape Resonances in superconducting gaps in a 2DEG at oxide-oxide interface. *J. Phys. Conf. Ser.* **2014**, *529*, 012007. [CrossRef]
13. Milosevic, M.V.; Perali, A. Emergent phenomena in multicomponent superconductivity: An introduction to the focus issue. *Supercond. Sci. Technol.* **2015**, *28*, 060201. [CrossRef]
14. Oya, G.; Koishi, M.; Sawada, Y. High-quality single-crystal Nb films and influences of substrates on the epitaxial growth. *J. Appl. Phys.* **1986**, *60*, 1440–1446. [CrossRef]
15. De Gennes, P.G. *Superconductivity of Metals and Alloys*; CRC Press: Boca Raton, FL, USA, 2013.
16. Pinto, N.; Rezvani, S.J.; Favre, L.; Berbezier, I.; Fretto, M.; Boarino, L. Geometrically induced electron-electron interaction in semiconductor nanowires. *Appl. Phys. Lett.* **2016**, *109*. [CrossRef]
17. Rezvani, S.J.; Pinto, N.; Enrico, E.; D'Ortenzi, L.; Chiodoni, A.; Boarino, L. Thermally activated tunneling in porous silicon nanowires with embedded Si quantum dots. *J. Phys. D Appl. Phys.* **2016**, *49*, 105104. [CrossRef]
18. Pinto, N.; Rezvani, S.J.; Perali, A.; Flammia, L.; Milošević, M.V.; Fretto, M.; Cassiago, C.; De Leo, N. Dimensional crossover and incipient quantum size effects in superconducting niobium nanofilms. *Sci. Rep.* **2018**, *8*, 4710. [CrossRef]
19. Chen, Y.J.; Shanenko, A.A.; Perali, A.; Peeters, F.M. Superconducting nanofilms: molecule-like pairing induced by quantum confinement. *J. Phys. Cond. Matter* **2012**, *24*, 185701. [CrossRef]

20. Palestini, F.; Strinati, G.C. Systematic investigation of the effects of disorder at the lowest order throughout the BCS-BEC crossover. *Phys. Rev. B* **2013**, *88*, 174504. [CrossRef]
21. Nannarone, S.; Borgatti, F.; DeLuisa, A.; Doyle, B.P.; Gazzadi, G.C.; Giglia, A.; Finetti, P.; Mahne, N.; Pasquali, L.; Pedio, M.; et al. The BEAR Beamline at Elettra. In *AIP Conference Proceedings*; AIP Publishing LLC: Melville, NY, USA, 2004; Volume 705, pp. 450–453. [CrossRef]
22. Pasquali, L.; De Luisa, A.; Nannarone, S. The UHV Experimental Chamber For Optical Measurements (Reflectivity and Absorption) and Angle Resolved Photoemission of the BEAR Beamline at ELETTRA. In *AIP Conference Proceedings*; AIP Publishing LLC: Melville, NY, USA, 2004; Volume 705, pp. 1142–1145. [CrossRef]
23. Rezvani, S.J.; Nobili, F.; Gunnella, R.; Ali, M.; Tossici, R.; Passerini, S.; Di Cicco, A. SEI Dynamics in Metal Oxide Conversion Electrodes of Li-Ion Batteries. *J. Phys. Chem. C* **2017**, *121*, 26379–26388. [CrossRef]
24. BEAR Beamline. Available online: https://www.elettra.trieste.it/it/lightsources/elettra/elettra-beamlines/bear/bear.html (accessed on 20 December 2018).
25. Lide, D.R. (Ed.) *Properties of Solids: Electrical Resistivity of Pure Metals*; CRC Press: Boca Raton, FL, USA, 2003.
26. Dean, J.A. (Ed.) *Electronic Configuration and Properties of the Elements*; McGraw-Hill: New York, NY, USA, 1999.
27. Hazra, D.; Datta, S.; Mondal, M.; Ghatak, J.; Satyam, P.V.; Gupta, A.K. Thickness dependent lattice expansion in nanogranular Nb thin films. *J. Appl. Phys.* **2008**, *103*, 103535. [CrossRef]
28. Hazra, D.; Mondal, M.; Gupta, A.K. Correlation between structural and superconducting properties of nano-granular disordered Nb thin films. *Phys. C Supercond. Appl.* **2009**, *469*, 268–272. [CrossRef]
29. Zhao, L.; Jin, Y.; Li, J.; Deng, H.; Li, H.; Huang, K.; Cui, L.; Zheng, D. Fabrication of Nb Superconducting Nanowires by Nanoimprint Lithography. *IEEE Trans. Appl. Supercond.* **2015**, *25*, 2200605. [CrossRef]
30. Delacour, C.; Ortega, L.; Faucher, M.; Fournier, T.; Pannetier, B.; Bouchiat, V. Persistence of superconductivity in niobium ultrathin films grown on R-plane sapphire. *Phys. Rev. B* **2011**, *83*, 144504–144508. [CrossRef]
31. Gubin, A.; Il'in, K.; Vitusevich, S.; Siegel, M.; Klein, N. Dependence of magnetic penetration depth on the thickness of superconducting Nb thin films. *Phys. Rev. B* **2005**, *72*, 064503–064508. [CrossRef]
32. Bose, S.; Raychaudhuri, P.; Banerjee, R.; Vasa, P.; Ayyub, P. Mechanism of the size dependence of the superconducting transition of nanostructured Nb. *Phys. Rev. Lett.* **2005**, *95*, 147003. [CrossRef] [PubMed]
33. Gershenzon, M.; Koshelets, V. Study of superconducting properties of Nb and NbN films obtained by method of high particle cathode atomization. *Zh. Tekh. Fiz.* **1980**, *50*, 572.
34. Bianconi, A.; MArcelli, A. *Synchrotron Radiation Research: Advances in Surface And Interface Science Techniques*; Springer: Boston, MA, USA, 1992; pp. 63–115.
35. Rezvani, S.; Pinto, N.; Perali, A.; Nannarone, S. Interfacial Nb oxidation on silicon oxide and sapphire studied by x-ray absorption and reflection spectroscopy. In preparation.
36. McMillan, W.L. Tunneling Model of the Superconducting Proximity Effect. *Phys. Rev.* **1968**, *175*, 537–542. [CrossRef]
37. Shanenko, A.A.; Croitoru, M.D.; Peeters, F.M. Quantum-size effects on T_C in superconducting nanofilms. *Europhys. Lett.* **2006**, *76*, 498–504. [CrossRef]